SCIENCE LETTERS

eISSN: 2682-8626

Available online at
http://myjms.mohe.gov.my/index.php/sl

Science Letters 18(2) 2024, 70 – 77.

Science Letters

Synthesis of Pristine Al_2O_3 Powder *Via* Self-Propagating Combustion Method with Various Fuel Sources

Missha Balqis Shariamin[1], Mas Fiza Mustafa[1], Mohd Sufri Mastuli[1,2], Annie Maria Mahat[1,2*]

[1]*Faculty of Applied Sciences, Blok C, Kompleks Sains 2, Universiti Teknologi MARA, 40450 Shah Alam, Selangor, Malaysia.*
[2]*Institute of Science, Level 3, Kompleks Inspirasi, Universiti Teknologi MARA, 40450 Shah Alam, Selangor, Malaysia.*

ARTICLE INFO

Article history:
Received 1 April 2024
Revised 28 May 2024
Accepted 1 June 2024
Online first
Published 24 June 2024

Keywords:
Al_2O_3
Structural
Oxidation
Thermal analysis
X-ray techniques

DOI:
10.24191/sl.v18i2.27018

ABSTRACT

In this study, pristine Al_2O_3 powder was prepared by a simple self-propagating combustion (SPC) method. The effect of the different fuels on synthesized Al_2O_3 powder on thermal, structural, and morphological properties was investigated. The fuels utilized include formic, citric, oxalic, and tartaric acids. Based on the STA results, all precursors were annealed at 1100ºC for 24 hours to obtain pristine Al_2O_3 powder. XRD results show that all samples correspond to the α-Al_2O_3 crystal structure. Notably, differences in the morphology and particle size of all samples were observed through FESEM micrographs.

INTRODUCTION

Aluminium oxide (Al_2O_3) is known to be the most widely used ceramic materials in various applications such as coating [1], catalyst [2], and electrical insulator [3]. Various applications were attributed to different phases of Al_2O_3, namely, gamma (γ), eta (η), theta (θ), and alpha (α). The transition of phases strongly depends on the preparation methods and experimental conditions. α-Al_2O_3 is the most stable phase, usually obtained at higher annealing temperatures (~1000ºC-1100ºC) [4, 5].

Various methods have been reported to produce Al_2O_3 powder, such as hydrothermal [6], sol-gel [7], co-precipitation [8], and combustion [5, 9]. Hydrothermal method requires high pressure and high-temperature autoclave, which is expensive, ineffective, and hazardous. Meanwhile, inexpensive and less hazardous methods such as sol-gel and co-precipitation are time-consuming due to their complex processes.

* Corresponding author. *E-mail address*: anniemaria@uitm.edu.my

Numerous studies have highlighted the self-propagating combustion (SPC) method as an effective and environmentally friendly approach for synthesizing pure Al_2O_3 materials, owing to its straightforward, rapid process [5, 10-12].

The SPC process requires precise control over several variables to regulate the Al_2O_3 powders' size, shape, structure, and thermal characteristics. These elements consist of fuel, starting materials, and heat treatment. The choice of fuel is crucial since it affects critical elements of combustion, such as temperature, reaction speed, and the composition of the finished product. The characteristics of the synthesized Al_2O_3, such as particle size, shape, and crystal structure, are similarly affected by the fuel selection [13, 14].

We have previously used the SPC approach to synthesize pure single-phase Al_2O_3 [5] successfully. Nevertheless, we found that different particle sizes and morphologies were produced when citric acid was used as a fuel. This was explained by the fact that citric acid caused a rather mild combustion process, which resulted in size and form. This finding emphasizes the necessity of investigating how various fuels affect the characteristics of Al_2O_3 powder produced using the SPC technique. Since every fuel has a different chemical structure, we expect different synthesis conditions for every fuel type. This drives us to use the SPC method to produce pure Al_2O_3 powder for different fuels: formic acid, citric acid, oxalic acid, and tartaric acid. To determine how each fuel affects the finished product, we will thoroughly examine the synthesized powder's combustion phenomena and thermal, structural, and morphological properties.

EXPERIMENTAL

In this experiment, aluminium nitrate nonahydrate ($Al(NO_3)_3.9H_2O$, formic acid (CH_2O_2), citric acid monohydrate ($C_6H_8O_7.H_2O$), Oxalic acid ($C_2H_2O_4$) and tartaric acid ($C_6H_6O_6$) were acting as starting materials. Formic acid, citric acid, oxalic acid, and tartaric acid act as fuels, and all synthesized Al_2O_3 samples were named after FA, CA, OA, and TA accordingly. Before synthesis, the amounts of metal salt and fuel were calculated to maximize chemical and energy release usage during combustion. The molar ratio of 1:1 between metal salt and fuel was applied for all starting materials to minimize the usage of starting materials. All synthesis processes were handled in a fume hood. For the synthesis of Al_2O_3, 73.6043g of $Al(NO_3)_3.9H_2O$ was dissolved with 40ml of deionized water and stirred by using a magnetic stirrer at room temperature until a clear solution was formed. 11 ml of CH_2O_2 was added to the solution under stirring. The stirring process continued until it became homogenous. Then, the mixture was heated on the hot plate at 350ºC until the combustion process occurred and the precursor was produced. The precursor was grounded until fine powder was obtained using mortar and pestle. From the graph of TG/DSC, the right annealing temperature to produce pure Al_2O_3 was obtained. All the processes were repeated for citric acid, oxalic acid, and tartaric acid. PANalyticalX'Pert-Pro MPD diffractometer with CU-K_α radiation as a beam source was used to obtain all samples' X-ray diffraction (XRD) patterns. The morphology was observed using a Field Emission Scanning Electron Microscope (FESEM).

RESULT AND DISCUSSION

Fig. 1 (a-d) shows the combustion phenomena of all samples prepared in the fume hood. For the similar heating temperature of 350ºC, it was found that the time taken for the combustion to occur varies for all samples. FA was found to combust easily within 72 min. This is expected to be simple organic acid formic acid [15]. CA took 150 min to combust; this was longer than FA, as citric acid is considered a more complex organic acid with a larger molecular structure [16]. Meanwhile, OA took 387 min to combust. Compared to CA, it is acceptable that it took more time to combust because oxalic acid has a simpler molecular structure than citric acid. Since citric acid has a more complex structure with six carbon atoms, it always has more potential sites for combustion. Hence, it is more prone to reacting with oxygen and undergoing combustion readily [17]. Furthermore, TA was found to have the longest time to combust; it

https://doi.org/10.24191/sl.v18i2.27018

took 1024 min; this could be attributed to a more complex molecule than tartaric acid. It contains four carbon atoms and six oxygen to access reactive sites and initiate combustion [18].

From the smoke observation, formic acid is shown in Fig. 1(a). produces thicker smoke than other fuels, indicating incomplete combustion due to insufficient oxygen gas supply. This is acceptable as formic acid (CH_2O_2) has the least oxygens compared to other fuels. As in Fig. 1(b), it is shown that citric acid results in fewer smoke-forming compounds. The complex structure of citric acid provides a higher proportion of carbon, hydrogen, and oxygen atoms, which eventually contribute to cleaner combustion. Also, with an oxygen-rich molecule structure, it undergoes more complete and efficient combustion [19]. Furthermore, as shown in Fig. 1(c) and (d), oxalic acid and tartaric acid produce more smoke than citric acid. This condition can result in more carbon-rich by-products, which are more likely to generate smoke [20].

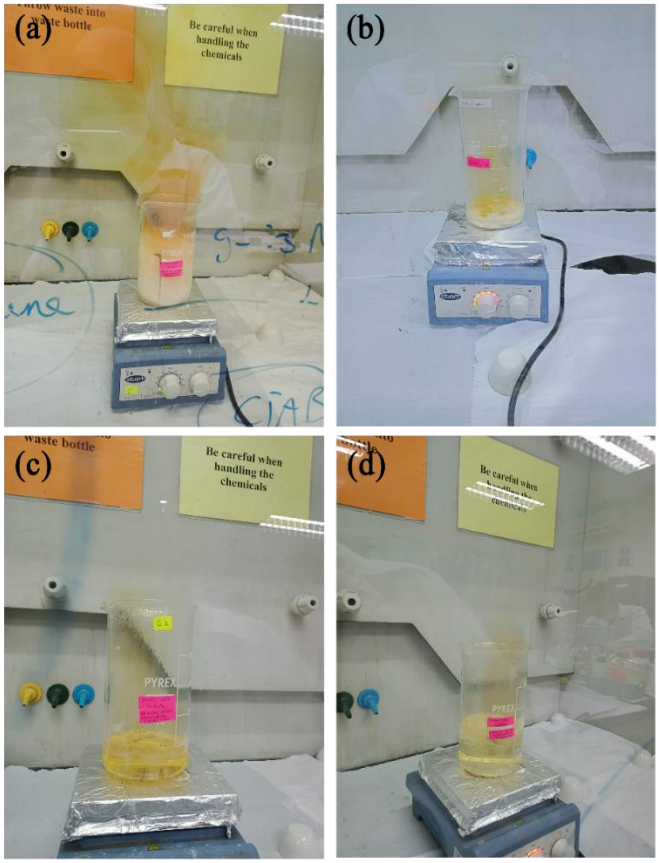

Fig. 1. Images of combustion phenomena of precursors during heating at 350ºC (a) FA, (b) CA, (c) OA, and (d) TA.

STA (TG-DSC) was performed for Al_2O_3 precursors in the range of 30ºC- 1200ºC. Fig. 2(a-d) shows the thermal analysis results of all samples. Significantly, all samples have different decomposition behavior. FA, CA, OA, and TA decomposition temperatures are 360ºC, 560ºC, 380ºC, and 680ºC, respectively. This indicated that the OH is difficult to remove by heating. As can be observed from the chemical formula of the citric acid monohydrate and tartaric acid, the number of OH is larger than formic acid and oxalic acid.

https://doi.org/10.24191/sl.v18i2.27018

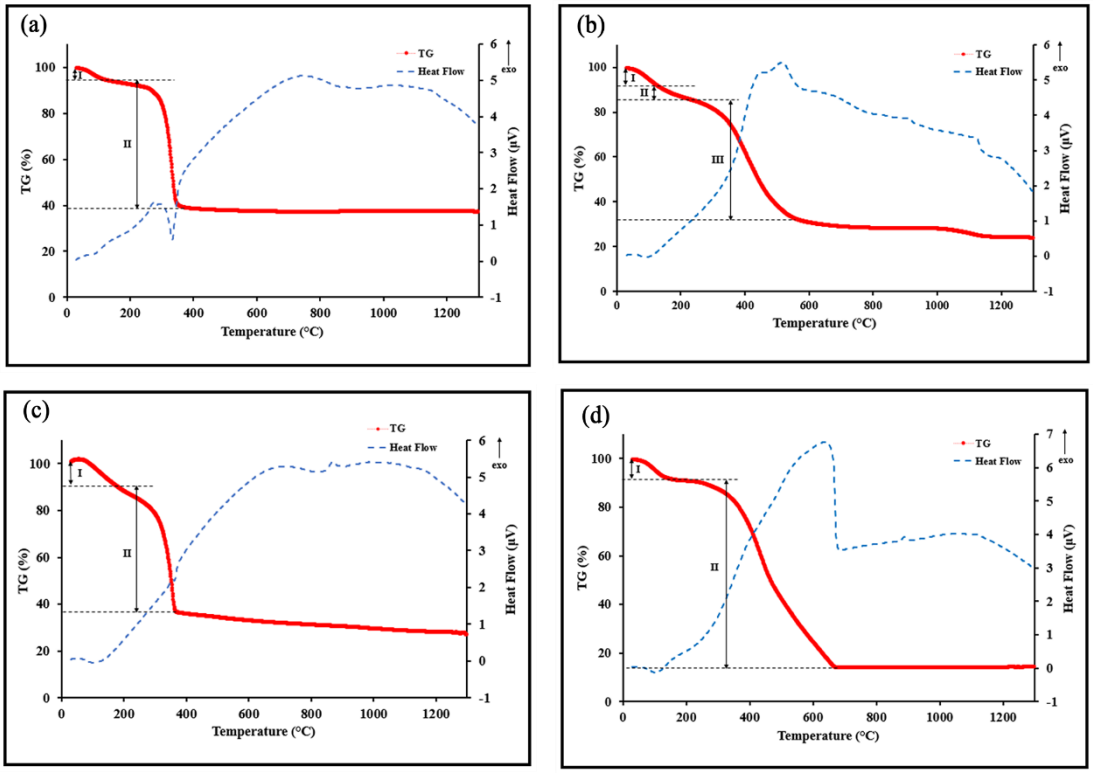

Fig. 2. TG/DSC curves of precursors (a) FA, (b) CA, (c) OA, and (d) TA.

FA's thermal profile (Fig. 2(a)) shows two regions that indicate the weight losses in the profile. Region I have weight loss of around 3.96% at a temperature range of 30ºC-100ºC. A huge weight loss occurred in region II at a temperature range of 100ºC-360ºC accompanied by an endothermic peak that indicates loss of water remaining in the precursor. As shown in Fig. 2(b), the thermal profile of CA has three distinct regions of weight loss. The weight loss in the region I am around 6.94% at a temperature range of 30ºC - 110ºC due to the evaporation of water. At Region II, the weight loss is about 8.48% at the temperature of 110ºC-250ºC. Region II shows the last weight loss of 51.26% at the temperature range of 250ºC-560ºC, accompanied by the exothermic reaction in producing the final product of Al_2O_3.

Fig. 2(c). shows the thermal profile of OA, which indicates the existence of two major regions of weight loss. Region I has a weight loss of around 11.86% at the temperature range of 30ºC-250ºC, indicating the loss of water that remained in the precursor. In Region II, the weight loss of about 50.77% at 250ºC-380ºC is attributed to the oxidation stage, where the pore gases release and oxygen absorption. Furthermore, as shown in Fig. 2(d)., the thermal profile of TA consists of two regions of weight loss. For region I, it has weight loss around 7.69% at a temperature range of 30ºC-100ºC. In Region II, a major weight loss of about 50.77% occurred at the temperature range of 100ºC-680ºC, which indicated the decomposition of the precursor and the formation of pure Al_2O_3.

Based on the TG profile of all fuels, the graph is stable at 700ºC onwards. Meanwhile, the DSC graph of OA and TA shows that an exothermic peak occurred at a temperature of 900ºC without any weight loss attributed to the phase transformation to produce pure Al_2O_3. At the temperature of 1100ºC onwards, the

https://doi.org/10.24191/sl.v18i2.27018

graph of DSC for all precursors shows that no more phase transformation occurred. Therefore, the annealing temperature of 1100ºC for 24 hours is chosen to obtain pure Al_2O_3.

Fig. 3. shows the XRD patterns of the samples. All peaks are indexed to the hexagonal crystal structure of the α-Al_2O_3 with space group R-3c, as confirmed by ICDD01-088-0826. The diffraction patterns show that all samples are in a single phase, indicating that highly pure α-Al_2O_3 is obtained. It is observed that small differences in intensities suggest that the crystalline structures of all synthesized samples are very similar. Hence, further confirmation by FESEM micrographs is adaptable for this condition.

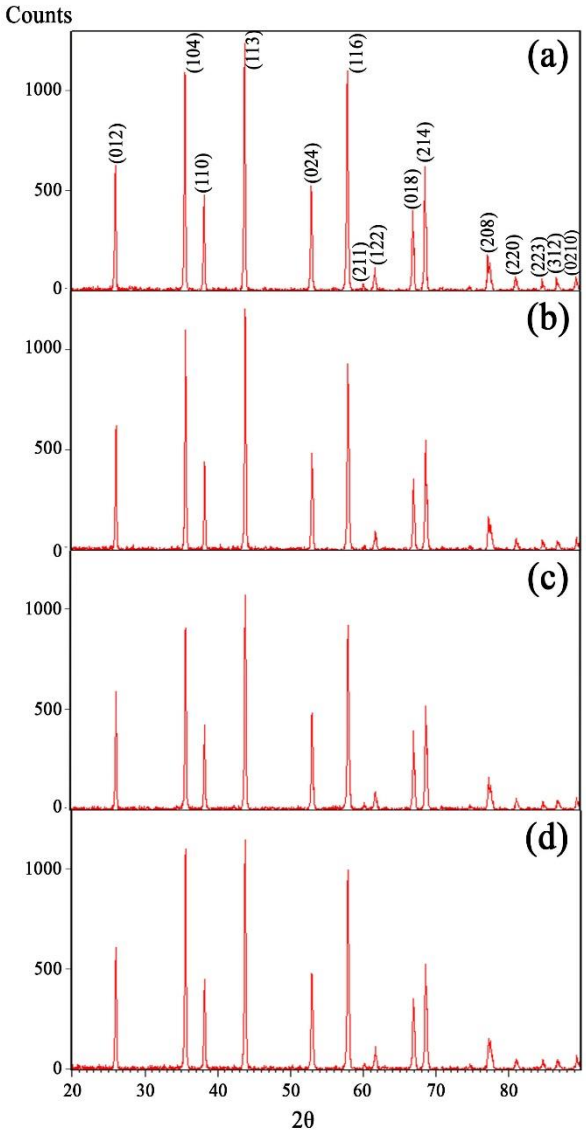

Fig. 3 XRD patterns of α-Al_2O_3 samples (a) FA, (b) CA, (c) OA, and (d) TA.

https://doi.org/10.24191/sl.v18i2.27018

From the FESEM images in Fig. 4., all samples are in the form of particles rather than crystallites. Between FA and TA, it was found that both samples showed reduced levels of agglomeration. This implies that the conditions governing crystal development and particle creation varied amongst the samples, which has been proven adaptable to the XRD intensities. Particularly, FA (~322nm) showed larger particles than TA (~282nm), suggesting a difference in the rate of crystal growth that permitted more significant particle development. However, OA (~241nm) displayed a higher degree of agglomeration despite having smaller particles than CA (~328nm). This is due to circumstances that promote nucleation above crystal development, which creates numerous tiny particles that eventually aggregate. These samples exhibit unique behaviors demonstrating the indicated interactions among nucleation rate, crystal growth, and the synthesis environment that affect particle size and agglomeration degree.

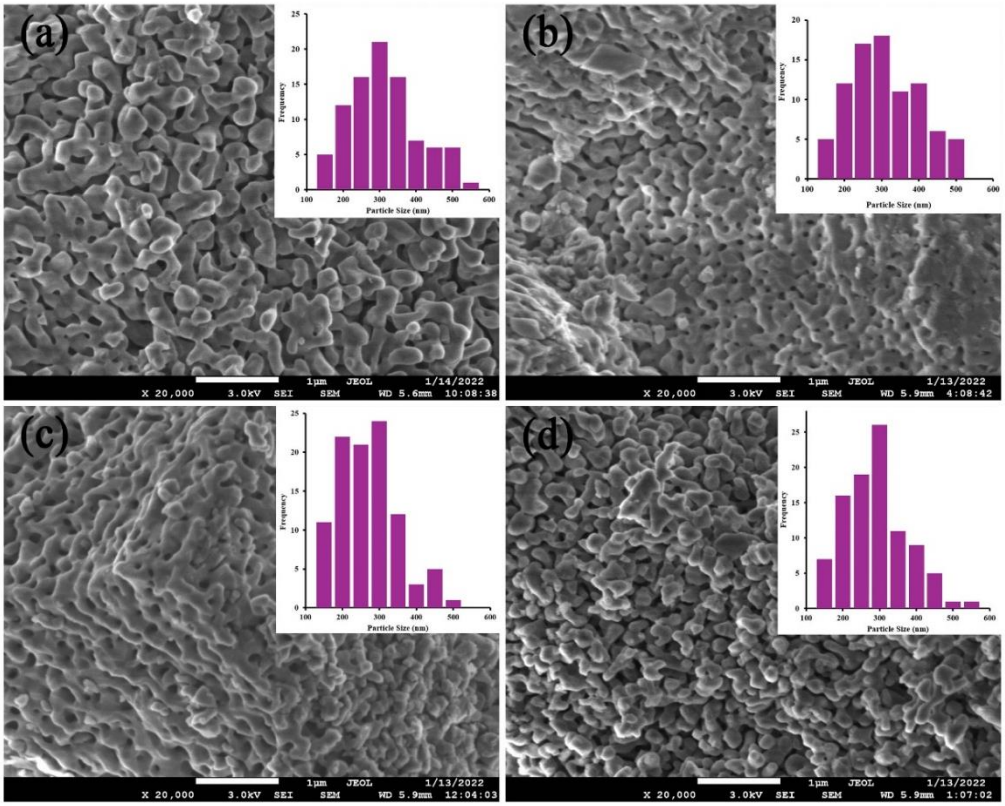

Fig. 4. FESEM micrographs of (a) FA, (b) CA, (c) OA, and (d) TA.

CONCLUSION

In this work, pristine α-Al_2O_3 is obtained *via* the SPC method using different fuels annealed at 1100ºC for 24 hours. Different fuels have different combustion behaviors in terms of their efficiency and speed of combustion. From the XRD results, all samples have small differences in intensities, and these were aligned with the results of FESEM micrographs. The observed significant variations in morphology among samples derived from different fuels present promising avenues for future studies to enhance functional and electrical performance.

https://doi.org/10.24191/sl.v18i2.27018

ACKNOWLEDGEMENTS/FUNDING

This work is financially supported by a Special Research Grant (GPK) from Universiti Teknologi MARA (Grant No.600-RMC/GPK 5/3 (140/2020).

CONFLICT OF INTEREST STATEMENT

The authors declare that there are no conflicts of interest regarding the publication of this manuscript.

AUTHORS' CONTRIBUTIONS

Missha Balqis Shariamin was involved in every stage of the research project. Missha was responsible for synthesizing the materials, conducting experiments, and collecting and analyzing data. Missha also contributed significantly to the manuscript's drafting and revision. Mas Fiza Mustafa assisted in data acquisition, providing support during experiments, data collection, and analysis. Mohd Sufri Mastuli, the co-supervisor, provided valuable guidance and oversight throughout the project. Mohd Sufri contributed to the study's conception and design, providing critical feedback on experimental methods and data interpretation. Annie Maria Mahat provided overarching supervision and direction for the project. Annie Maria was involved in the conceptualization of the research, provided resources and expertise, guided data interpretation, and contributed to the critical review and finalization of the manuscript.

REFERENCES

[1] M. H. Zare, N. Hajilary and M. Rezakazemi, "Microstructural modifications of polyethylene glycol powder binder in the processing of sintered alpha alumina under different conditions of preparation," *Materials Science for Energy Technologies,* vol. 2, pp. 89-95, 2019.

[2] A. P. Amrute, K. Jeske, Z. Łodziana, G. Prieto and F. Schüth, "Hydrothermal Stability of High-Surface-Area α-Al2O3and Its Use as a Support for Hydrothermally Stable Fischer-Tropsch Synthesis Catalysts," *Chemistry of Materials,* vol. 32, no. 10, pp. 4369-4374, 2020.

[3] P. Junge, c. Rupprecht, M. Greinacher, D. Kober and P. Stargardt, "Thermally Sprayed Al2O3 Ceramic Coatings for Electrical Insulation Applications," *Proceedings from the International Thermal Spray Conference.*

[4] P. Nayar, S. Waghmare, P. Singh, M. Najar, S. Puttewar and A. Agnihotri,, "Comparative study of phase transformation of Al2O3 nanoparticles prepared by chemical precipitation and sol-gel auto combustion methods," *Materials Today: Proceedings,* vol. 26, pp. 122-125, 2018.

[5] A. M. Mahat, N. Kamarulzaman, M. S. Mastuli, N. Badar, N. A. Jani and M. F. Omar, "Mechanism of the formation of novel Al2-xHfxO3 materials via a combustion synthesis method," *Results in Materials,* vol. 6, pp. 1-8, 2020.

[6] A. Y. Nalivaiko, A. N. Arnautov, S. V. Zmanovsky, D. Y. Ozherelkov, P. K. Shurkin and A. A. Gromov, "Al–Al2O3 powder composites obtained by hydrothermal oxidation method: Powders and sintered samples characterization," *Journal of Alloys and Compounds,* vol. 825, pp. 1-6, 2020.

https://doi.org/10.24191/sl.v18i2.27018

[7] A. A. Mohammed, Z. T. Khodair and A. A. Khadom, "Preparation and investigation of the structural properties of α-Al2O3 nanoparticles using the sol-gel method," *Chemical Data Collections,* vol. 29, pp. 1-8, 2020.

[8] R. Bharthasaradhi and L. C. Nehru, "Structural and phase transition of α- Al2O3 powders obtained by co-precipitation method," *Phase Transitions,* vol. 89, no. 1, pp. 77-83, 2016.

[9] A. M. Mahat, M. S. Mastuli and N. Kamarulzaman, "Influence of annealing temperature on the phase transformation of Al2O3," *AIP Conference Proceedings,* 2016.

[10] A. S. Patil, A. V. Patil, C. G. Dighavkar, V. A. Adole and U. J. Tupe, "Synthesis techniques and applications of rare earth metal oxides semiconductors: A review," *Chemical Physics Letters,* p. 796, 2022.

[11] X. Xu, R. Lai, C. Jiang, W. Zhang, L. Liu and G. Cao, "Self-propagating combustion synthesis of few-layer graphene for supercapacitors from CO and Mg," *Journal of Alloys and Compounds,* vol. 908, pp. 1-7, 2022.

[12] N. S. B. Saharin, N. E. Ahmad and A. R. Tamuri, "Thermoluminescence study of aluminium oxide doped germanium prepared by combustion synthesis method," *EPJ Web of Conferences,* vol. 156, pp. 1-7, 2017.

[13] R. Abbas , K. D. Martinson, T. Y. Kiseleva, G. P. Markov, P. Y. Tyapkin and V. I. Popkov, "Effect of fuel type on the solution combustion synthesis, structure, and magnetic properties of YIG nanocrystals," *Materials Today Communications,* vol. 32, pp. 1-7, 2022.

[14] E. Carlos, R. Martins, E. Fortunato and R. Branquinho, "Solution Combustion Synthesis: Towards a Sustainable Approach for Metal Oxides," *Chemistry - A European Journal,* vol. 26, no. 42, pp. 9099-9125, 2020.

[15] A. Rahbari, M. Ramdin, L. J. P. Van Den Broeke and T. J. H. Vlugt, "Combined Steam Reforming of Methane and Formic Acid to Produce Syngas with an Adjustable H2:CO Ratio," *Industrial and Engineering Chemistry Research,* vol. 57, no. 31, pp. 10663-10674, 2018.

[16] G. Yin, Q. Gao, E. Hu, J. Xu, M. Zhou and Z. Huang, "Experimental and kinetic study on laminar flame speeds of formic acid," *Combustion and Flame,* vol. 220, pp. 73-81, 2020.

[17] C. Qiu, L. Jiang, Y. Gao and L. Sheng, "Effects of oxygen-containing functional groups on carbon materials in supercapacitors: A review," *Materials and Design,* p. 230, 2023.

[18] H. Zhang, X. Chen, T. Xie, B. Yuan, H. Dai, S. He and X. Liu, "Effects of reduced oxygen levels on flame propagation behaviors of starch dust deflagration," *Journal of Loss Prevention in the Process Industries,* vol. 54, pp. 146-152, 2018.

[19] L. Li, S. Wang, L. Zhao and A. Fan, "A numerical investigation on non-premixed catalytic combustion of $CH_4/(O_2 + N_2)$ in a planar micro-combustor," *Fuel,* vol. 255, 2019.

[20] Q. Zhang, J. Zhan, K. Zhou, H. Lu, W. Zeng, A. A. Stec, T. R. Hull, Y. Hu and Z. Gui, "The influence of carbon nanotubes on the combustion toxicity of PP/intumescent flame retardant composites," *Polymer Degradation and Stability,* vol. 115, pp. 38-44, 2015.

https://doi.org/10.24191/sl.v18i2.27018